Supplementary Materials

In this Supplemental Information to *Carbon Storage and Enhanced Oil Recovery in Pennsylvanian Morrow Formation Clastic Reservoirs: Controls on Oil/Brine and Oil/CO2 Relative Permeability from Diagenetic Heterogeneity and Evolving Wettability* (text) by Rasmussen et al., we provide additional detail from µCT analysis of Morrow B sandstone HFUs, and data used in the calculation of absolute and relative permeability values from experimental measurements.

SM-1. Pore statistics determined from X-ray CT imaging and analysis.

To accompany Figure 7 in the text, which plot histograms of framework grain size determined from analysis of µCT tomographic reconstructions of Morrow B core plugs, in Figure S1 we

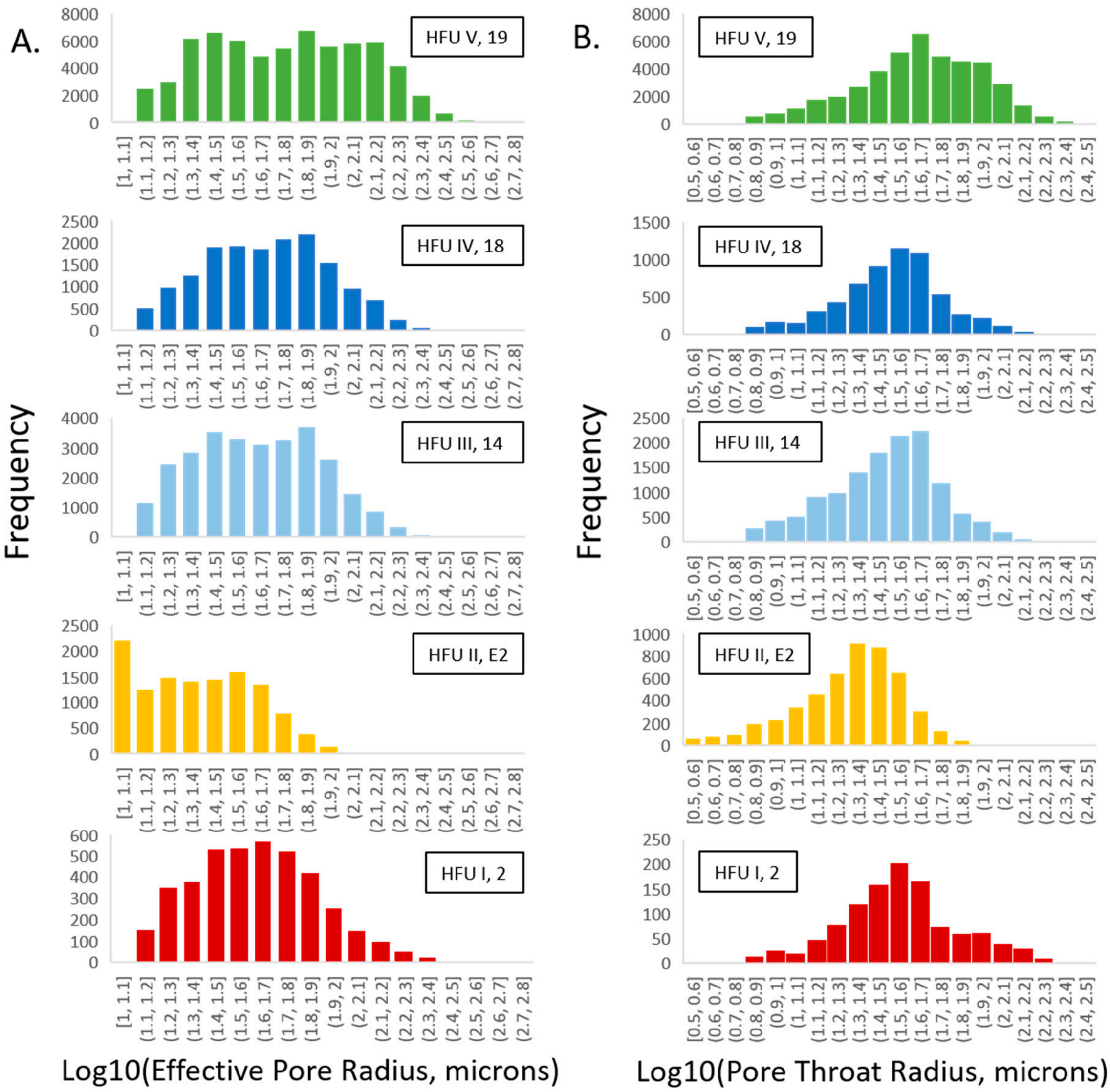

Figure S1. Pore radii and pore throat radii statistics for Morrow B HFUs determined from µCT image analysis using the Pergeos™ software suite. The color coding is the same used to reference HFUs in Figure 2 in the text. Number ranges for the abscissa histograms are given in log-base 10 of lengths in microns.

plot histograms of pore size and pore throat distributions of macro-pores resolvable by our methods. These are color coded by HFU, to match that used in Figure 2 of the text. HFU V has the largest pores in the Morrow B samples, while HFU II has the smallest (this HFU II sample is sample E2 in Table A1 in the text). While the HFU I sample has pore radii similar to those of higher HFUs, pores of this sample are largely occluded by carbonate cement, which explains why the pore count in the histogram frequency is much lower than the other HFUs. Pore throat radii systematically decrease with decreasing HFU number, with HFU V containing the most pores with the greatest value in pore throat radius. The sole exception is again HFU I, which has the fewest pore throats imaged in the HFU data sets.

Figure S2 plots frequency histograms of coordination number between only macro-pores and that considering macro-pores and microporous domains together. For HFU V, there is a slightly

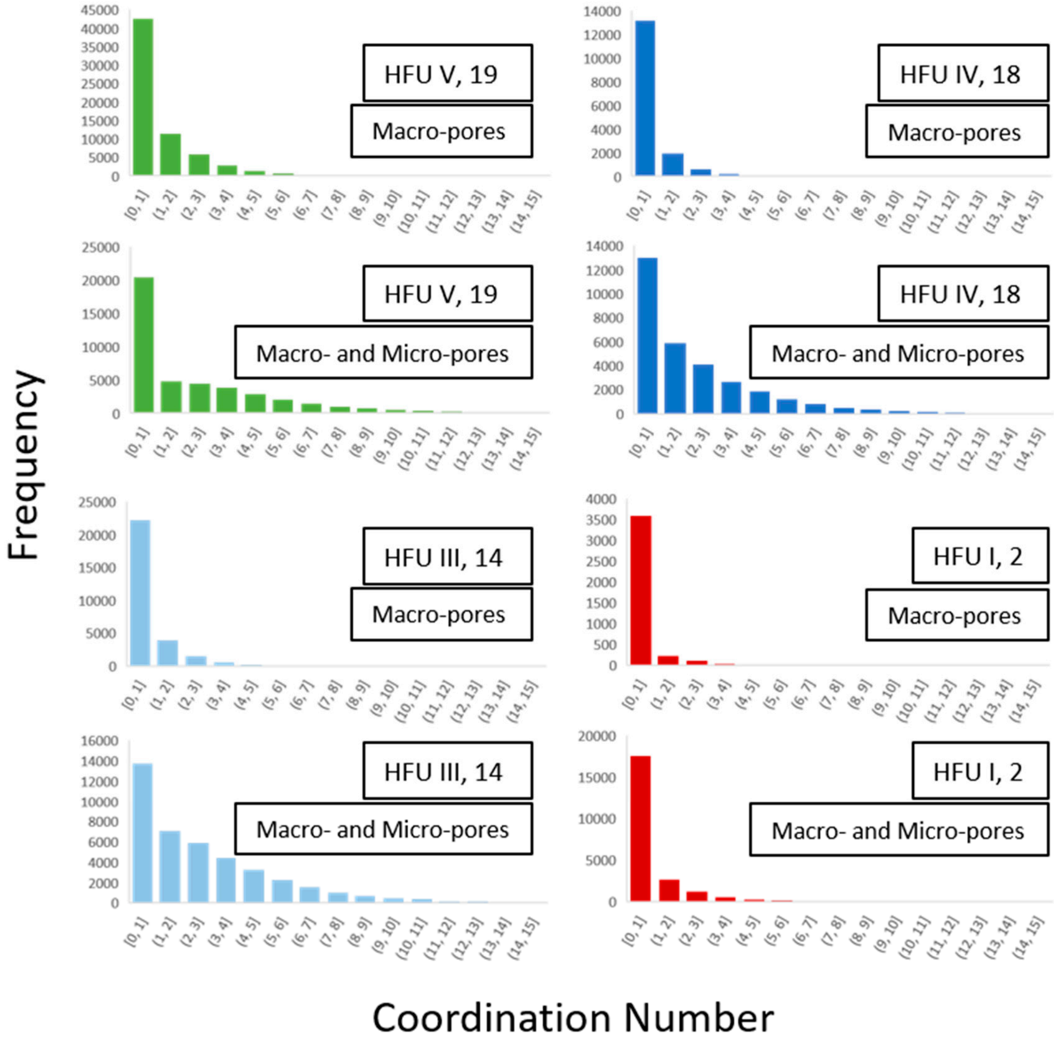

Figure S2. Coordination number between connected macro-pores, and between macro-pores and microporous regions. The color coding is the same used to reference HFUs in Figure 2 in the text.

greater frequency of connected macro-pores and microporous domains compared to just macro-pore connectivity, but there is a far greater difference between the two observed for HFU IV and HFU III. This shows that transport pathways for HFU III and IV samples must include microporous regions, which surround increasingly isolated macro-pores in going from HFU IV to HFU III. Pore coordination numbers are calculated using the "Pore Network Module" of the Pergeos^{TM} software suite. Pores for HFU I are largely isolated, again due to abundant carbonate cement. This shows that diagenetic processes, including secondary micro-porosity in clay-rich regions generated by feldspar dissolution, and pores largely occluded by carbonate cement, have a first-order effect on transport properties of the Morrow B HFUs examined in the text.

SM-2. Single-phase oil permeability of HFUs as a function of effective pressure.
Prior to the initial relative permeability experiment for each HFU core plug described in the text, and after the aging process, single phase oil permeability was measured as a function of effective pressure, beginning with a small initial effective pressure and ending at in situ effective pressures of 27.6 MPa. This was accomplished by maintaining a constant downstream pore pressure of 27.6 MPa and increasing confining pressure in steps. Together with a temperature of 76.0ºC, the final permeability at effective pressure of 27.6 MPa matches the in situ conditions of the Morrow B reservoir surrounding well 13-10A at Farnsworth. The data used in constructing Figure S3 are given in Table SI-1. The values of permeability at the maximum effective pressure are plotted via the 'x' symbol in Figure 2 of the text.

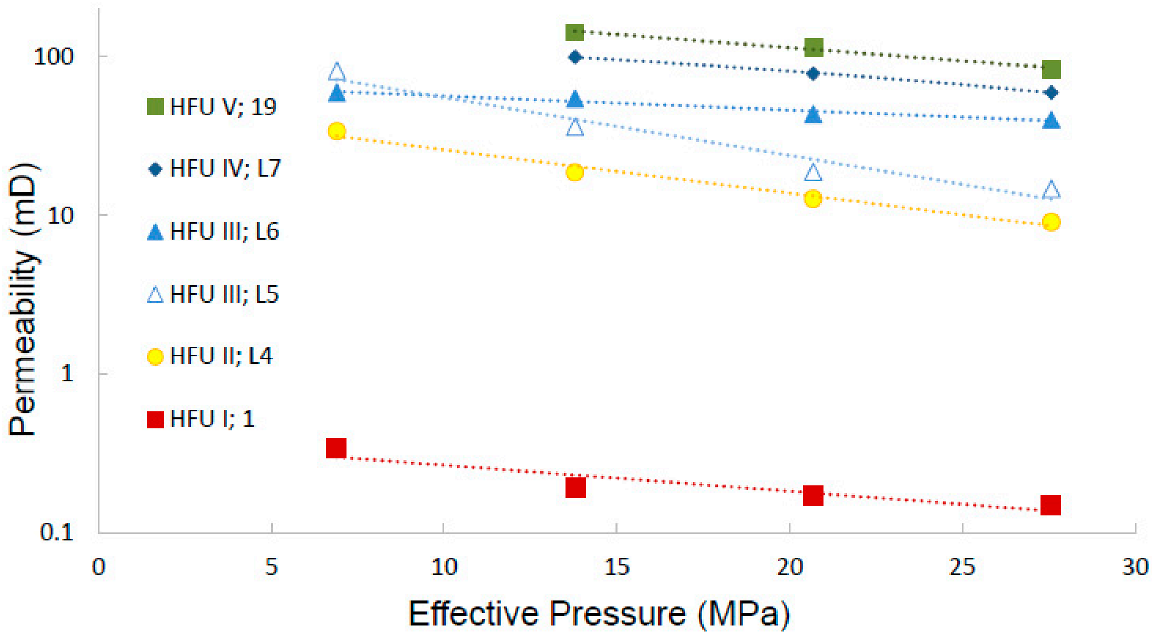

Figure S3. Single phase oil permeability as a function of effective pressure, for all core plugs used in relative permeability experiments described in the text. Colors correspond to different HFUs as used in Figure S1 and S2, and as used in the text. The absolute permeability decreases systematically from HFU V through I, and each HFU displays a linear decrease with effective pressure when plotted in semi-log space.

Table S-1. Conditions and values of single-phase oil permeability for Morrow B HFU core plugs plotted in Figure S3.

Sample	Effective Pressure (MPa)	Temperature (˚C)	Viscosity (cP)	Flow Rate (ml/min)	Δ P Core (MPa)	Permeability (mD)
19	13.790	76.0	1.66	1.98	0.066	99.6
19	20.684	76.0	1.66	1.98	0.084	78.3
19	27.579	76.0	1.66	1.98	0.110	59.5
L7	13.790	76.0	0.40	1.02	0.066	99.6
L7	20.684	76.0	0.40	1.02	0.084	39.1
L7	27.579	76.0	0.40	1.02	0.110	29.8
L6	6.895	76.0	1.66	1.02	0.456	59.4
L6	13.790	76.0	1.66	1.02	0.498	54.5
L6	20.684	76.0	1.66	1.02	0.624	43.5
L6	27.579	76.0	1.66	1.02	0.677	40.1
L5	6.895	76.0	1.66	0.78	0.248	81.6
L5	13.790	76.0	1.66	0.78	0.558	36.3
L5	20.684	76.0	1.66	0.48	0.717	18.8
L5	27.579	76.0	1.66	0.48	0.917	14.7
L4	6.890	76.0	1.66	1.50	1.103	33.9
L4	13.790	76.0	1.66	1.50	2.006	18.6
L4	20.684	76.0	1.66	1.50	2.944	12.7
L4	27.579	76.0	1.66	1.50	4.130	9.06
1	6.890	76.0	1.66	0.06	3.799	0.341
1	13.790	76.0	1.66	0.06	6.688	0.194
1	20.684	76.0	1.66	0.06	7.564	0.171
1	27.579	76.0	1.66	0.06	8.701	0.149

SM-3. Supplemental data for relative permeability experiments.

Data used in plotting Figures 12 and 13 in the text are given in Tables S2 and S3 below. This includes the measured pressure gradient across the pressure taps, non-oil phase saturation measured by mass balance, values of relative permeability of the two phases corresponding to the saturation value, and the calculated three-phase permeability used in the modeling of Sub-Section 4.5 in the text. Table S2 contains all relevant data for the oil and brine two phase co-injection experiments, and Table S3 contains all relevant data for the CO_2 and brine co-injection experiments.

Table S2. Pressure gradients, saturations, and relative permeability values used in plotting Figure 12 in the text for all oil and brine co-injection experiments.

Oil and Brine Experiments:									
Core 19 (HFU 5)					Core L7 (HFU 4)				
dP (MPa)	S_w	k_{rw}	k_{ro}	$k_{ro: \text{Three-Phase}}$	dP (MPa)	S_w	k_{rw}	k_{ro}	$k_{ro: \text{Three-Phase}}$
0.14	0.20	0.00	1.00	0.93	0.34	0.33	0.00	1.00	0.90
0.20	0.26	0.02	0.62	0.51	0.39	0.38	0.02	0.77	0.58
0.25	0.33	0.03	0.46	0.33	0.63	0.42	0.03	0.43	0.27
0.59	0.39	0.03	0.16	0.10	0.74	0.46	0.03	0.32	0.16
0.43	0.45	0.03	0.19	0.09	0.95	0.50	0.03	0.21	0.08
0.52	0.52	0.03	0.14	0.55	0.89	0.55	0.05	0.19	0.06
0.61	0.58	0.03	0.09	0.04	1.01	0.59	0.05	0.13	0.04
0.69	0.64	0.03	0.06	0.02	1.04	0.63	0.05	0.10	0.03
0.69	0.71	0.04	0.04	0.02	0.90	0.72	0.08	0.04	0.03
0.57	0.77	0.05	0.02	0.03	0.38	0.76	0.21	0.00	0.00
0.37	0.83	0.09	0.00	0.00					

Core L5 (HFU 3)					Core L6 (HFU 3)				
dP (MPa)	S_w	k_{rw}	k_{ro}	$k_{ro: \text{Three-Phase}}$	dP (MPa)	S_w	k_{rw}	k_{ro}	$k_{ro: \text{Three-Phase}}$
2.33	0.38	0.00	1.00	1.00	1.28	0.44	0.00	1.00	1.00
3.92	0.41	0.01	0.40	0.37	2.50	0.47	0.01	0.46	0.30
5.63	0.45	0.01	0.25	0.22	3.04	0.50	0.02	0.34	0.14
7.04	0.48	0.02	0.17	0.12	3.73	0.53	0.02	0.24	0.05
8.37	0.52	0.02	0.13	0.08	4.05	0.56	0.03	0.19	0.02
9.81	0.56	0.02	0.09	0.05	4.36	0.58	0.04	0.15	0.01
10.14	0.59	0.02	0.07	0.04	4.23	0.61	0.04	0.12	0.01
11.68	0.63	0.03	0.04	0.03	4.57	0.64	0.05	0.08	0.01
11.99	0.67	0.03	0.03	0.03	4.67	0.67	0.05	0.05	0.02
10.23	0.70	0.04	0.02	0.04	4.65	0.70	0.06	0.03	0.04
4.12	0.74	0.10	0.00	0.00	1.66	0.73	0.19	0.00	0.00

Core L4 (HFU 2)					Core 1 (HFU 1)				
dP (MPa)	S_w	k_{rw}	k_{ro}	$k_{ro: Three-Phase}$	dP (MPa)	S_w	k_{rw}	k_{ro}	$k_{ro: Three-Phase}$
2.96	0.45	0.00	1.00	1.00	5.44	0.37	0.00	1.00	1.00
4.72	0.47	0.02	0.57	0.27	4.53	0.48	0.09	0.84	0.23
6.76	0.49	0.02	0.35	0.12	3.59	0.62	0.26	0.45	0.01
8.97	0.54	0.03	0.20	0.02	7.15	0.73	0.18	0.00	0.00
8.97	0.56	0.04	0.17	0.02					
10.05	0.58	0.04	0.12	0.02					
12.52	0.60	0.04	0.07	0.02					
12.10	0.62	0.05	0.05	0.02					
10.23	0.64	0.06	0.03	0.01					
4.30	0.66	0.17	0.00	0.00					

Table S3. Pressure gradients, saturations, and relative permeability values used in plotting Figure 13 in the text for all oil and CO_2 co-injection experiments.

Oil and Gas Experiments: Core 19 (HFU5)											
Outlet Pressure 20.68 MPa				Outlet Pressure 24.82 MPa				Outlet Pressure 27.58 MPa			
dP (MPa)	S_g	k_{rg}	k_{ro}	dP (MPa)	S_g	k_{rg}	k_{ro}	dP (MPa)	S_g	k_{rg}	k_{ro}
1.72	0.19	0.00	1.00	11.72	0.15	0.00	1.00	11.05	0.13	0.00	1.00
2.31	0.26	0.00	0.67	11.43	0.22	0.00	0.92	15.24	0.20	0.00	0.33
2.08	0.32	0.01	0.66	10.53	0.29	0.01	0.89	13.71	0.27	0.00	0.32
1.92	0.39	0.01	0.63	9.14	0.36	0.01	0.90	12.69	0.35	0.01	0.30
1.92	0.45	0.01	0.54	8.55	0.43	0.02	0.82	11.99	0.49	0.01	0.23
1.54	0.51	0.02	0.56	6.97	0.50	0.03	0.84	9.69	0.57	0.01	0.23
1.16	0.58	0.03	0.59	9.98	0.57	0.03	0.47	9.38	0.64	0.02	0.18
6.74	0.64	0.01	0.08	10.40	0.64	0.03	0.34	8.77	0.71	0.02	0.13
8.27	0.71	0.01	0.04	8.94	0.71	0.04	0.26	6.89	0.79	0.03	0.08
8.40	0.77	0.01	0.02	9.76	0.77	0.04	0.12	1.50	0.86	0.14	0.00
1.13	0.84	0.06	0.00	3.12	0.84	0.14	0.00				

Oil and Gas Experiments: Core L5 (HFU3)											
Outlet Pressure 20.68 MPa				Outlet Pressure 24.82 MPa				Outlet Pressure 27.58 MPa			
dP (MPa)	S_g	k_{rg}	k_{ro}	dP (MPa)	S_g	k_{rg}	k_{ro}	dP (MPa)	S_g	k_{rg}	k_{ro}
6.62	0.09	0.00	1.00	7.73	0.18	0.00	1.00	7.29	0.13	0.00	1.00
7.91	0.16	0.00	0.75	8.56	0.24	0.00	0.81	12.35	0.20	0.00	0.89
8.20	0.23	0.01	0.65	8.69	0.30	0.01	0.71	11.86	0.27	0.01	0.82
8.10	0.30	0.01	0.57	8.75	0.36	0.01	0.62	12.30	0.34	0.01	0.69
5.56	0.36	0.02	0.71	7.21	0.42	0.02	0.64	11.68	0.41	0.02	0.62
4.97	0.43	0.03	0.67	6.57	0.48	0.02	0.59	11.67	0.48	0.02	0.52
10.62	0.50	0.01	0.25	10.68	0.54	0.02	0.29	9.30	0.55	0.03	0.52
10.76	0.57	0.02	0.18	10.99	0.60	0.02	0.21	12.02	0.62	0.03	0.30

10.54	0.63	0.02	0.13	9.80	0.66	0.02	0.16	11.42	0.69	0.03	0.21
8.97	0.70	0.03	0.07	8.72	0.72	0.03	0.09	11.20	0.76	0.04	0.11
5.65	0.77	0.04	0.00	1.69	0.78	0.18	0.00	3.29	0.82	0.14	0.00